ELSEVIER

Catalysis Today 60 (2000) 11–20

CATALYSIS TODAY

www.elsevier.com/locate/cattod

Simplified method of effectiveness factor calculations for irregular geometries of washcoats A general case in a 3D concentration field

D. Papadias [a,*], L. Edsberg [b], P. Björnbom [a]

[a] *Department of Chemical Engineering and Technology, Chemical Reaction Engineering, KTH Royal Institute of Technology, Teknikringen 42, S-100 44 Stockholm, Sweden*

[b] *Department of Numerical Analysis and Computing Science, KTH Royal Institute of Technology, Teknikringen 42, S-100 44 Stockholm, Sweden*

Abstract

A simplified 3D-model for isothermal conditions has been developed to reduce the calculations of the combined rate of pore diffusion and chemical reaction in washcoats of irregular geometries. The method is based on sectioning the washcoat into particles thus treating the solid-phase according to a corresponding boundary value problem. The simplified 3D-model was compared with a rigorous model for five different geometrical configurations of a square monolith with uneven washcoat coating. For the first and power law (0.7th order) kinetics the solutions of the reduced model were in very good agreement in comparison with the more expensive 3D-model. The computational burden could be even further reduced by using a lumped model in spite of peripherally varying concentration profiles. The agreement using the lumped model was satisfactory whenever proper correlations for the mass-transfer coefficient and the effectiveness factor were used.

Keywords: Effectiveness factor; Washcoats; 3D-models

1. Introduction

Monolithic reactors have received much interest over the past decades in pollution control applications with examples such as the three-way catalyst, SCR catalytic converters for NO_x-control and the current development of catalytic fuel combustion [1–3]. Mathematical modelling and reactor simulations play an important role as tools to understand the complex relationships in the catalytic chamber and to determine an optimal reactor design.

A number of efforts have been devoted to modelling monolith reactors with various degrees of sophistication [4–6]. A trade-off between the difficulties in solving the model and the accuracy of the modelling results is usually necessary since sophisticated models of chemical reactors most often are too difficult to solve. The degree of complexity of the mathematical treatment can be assessed by comparing simpler models with more comprehensive ones in order to address model simplifications and adequacy of the simplified approach [6].

A frequent approximation when modelling monolithic reactors is to assume a uniform, flat coating of washcoat in the monolith. However, the assumption of a perfectly uniformly distributed washcoat can

* Corresponding author. Tel.: +46-8-790-82-51; fax: +46-8-10-85-79.
E-mail address: dennis@ket.kth.se (D. Papadias)

0920-5861/00/$ – see front matter
PII: S0920-5861(00)00312-6

overestimate the heterogeneous reaction rate markedly since diffusion limitations become severe in the corner of the channel due to non-uniform coating [7,8]. In a recent investigation at our laboratory, a simplified method was developed to a priori address the effectiveness factor in non-uniform washcoats [9]. The study considered a two-dimensional flow field in the monolith channel giving a uniform concentration around the wall perimeter. Our simplified method consists of a symbolic sectioning of the washcoat into particles treating the analysis of diffusion and reaction in irregular shapes of coating in a one-dimensional case.

In practice, however, an active coating with varying thickness around the perimeter of the monolith channel would necessitate a three-dimensional concentration field when modelling the flow and the catalytic reaction in the whole reactor channel. The surface concentration on the wall of the washcoat would therefore vary along this perimeter. In the present study, a more general case of the results in our previous work is examined in a three-dimensional concentration field of the monolith channel. Three-dimensional reactor simulations in a monolith channel combined with equations for the washcoat are compared with the case where an individual effectiveness factor based on the individual surface concentration for each washcoat segment is calculated. The simpler approach reduces the differential equations of the washcoat to a corresponding boundary value problem giving significant savings in computational time. In this paper, the methodology of the simplified 3D-modelling is developed and validated under isothermal conditions. A comparison of the 3D-solutions with simpler geometrical models is also addressed to investigate whether the computational burden can be further reduced.

2. Theory

We will investigate the modelling of an isothermal monolith reactor with one reaction. Our results may be relevant in connection with, e.g. low temperature oxidation of VOC in monolith reactors. We anticipate that our results can be extended, and are planning to do so, to multiple reaction systems, e.g. SCR reactors.

Five different geometrical cross-sections for the monolith channel were used, of which the first four are defined in Fig. 1. The last cross-section consists of a uniform catalyst layer on a square monolith channel as an asymptotic case. The first geometrical shape, GI, consists of a circular washcoat with a minimum thickness of 20 μm. This minimum thickness gets broader in the other geometries (GII–GIV) as the fillet radius in the corner of the monolith is decreased. Assumptions for the modelling of the different monolithic patterns, which are considered relevant for this study, are:

- steady-state and isothermal conditions;
- identical properties in all monolith channels;
- fully developed laminar flow at the inlet of the channels;
- neglect of axial molecular diffusion in the gas-phase.

Two different kinds of kinetic equations were used in this study, a first order reaction rate and a non-linear power law. The governing equations for the more rigorous formulation of the monolith channel consider the material balance both in the gas-phase and the washcoat. The general equations in rescaled form are in Section 2.1, with symbols defined in Section 4.

2.1. 3D-model in two domains

Gas-phase

$$\left[\frac{U(x,y)R_{\mathrm{m}}^2}{LD_{\mathrm{g}}}\right]\frac{\partial\Psi}{\partial z}=\left(\frac{\partial^2\Psi}{\partial x^2}+\frac{\partial^2\Psi}{\partial y^2}\right) \tag{1}$$

Solid-phase

$$\left(\frac{\partial^2\Psi}{\partial x^2}+\frac{\partial^2\Psi}{\partial y^2}\right)-\left(\frac{R_{\mathrm{m}}^2 k_{\mathrm{c0}} C_{\mathrm{f0}}^{n-1}}{D_{\mathrm{e}}}\right)\Psi^n=0 \tag{2}$$

A uniform concentration at the channel inlet is used (Ψ=1 at z=0). The boundary conditions are zero flux at lines of symmetry and on the washcoat surface towards the monolith channel. At the interface between the gas-phase and the solid-phase the flux boundary equation is

$$\left(D_{\mathrm{g}}\frac{\partial\Psi}{\partial n}\right)_{\Gamma}=\left(D_{\mathrm{e}}\frac{\partial\Psi}{\partial n}\right)_{\Gamma} \tag{3}$$

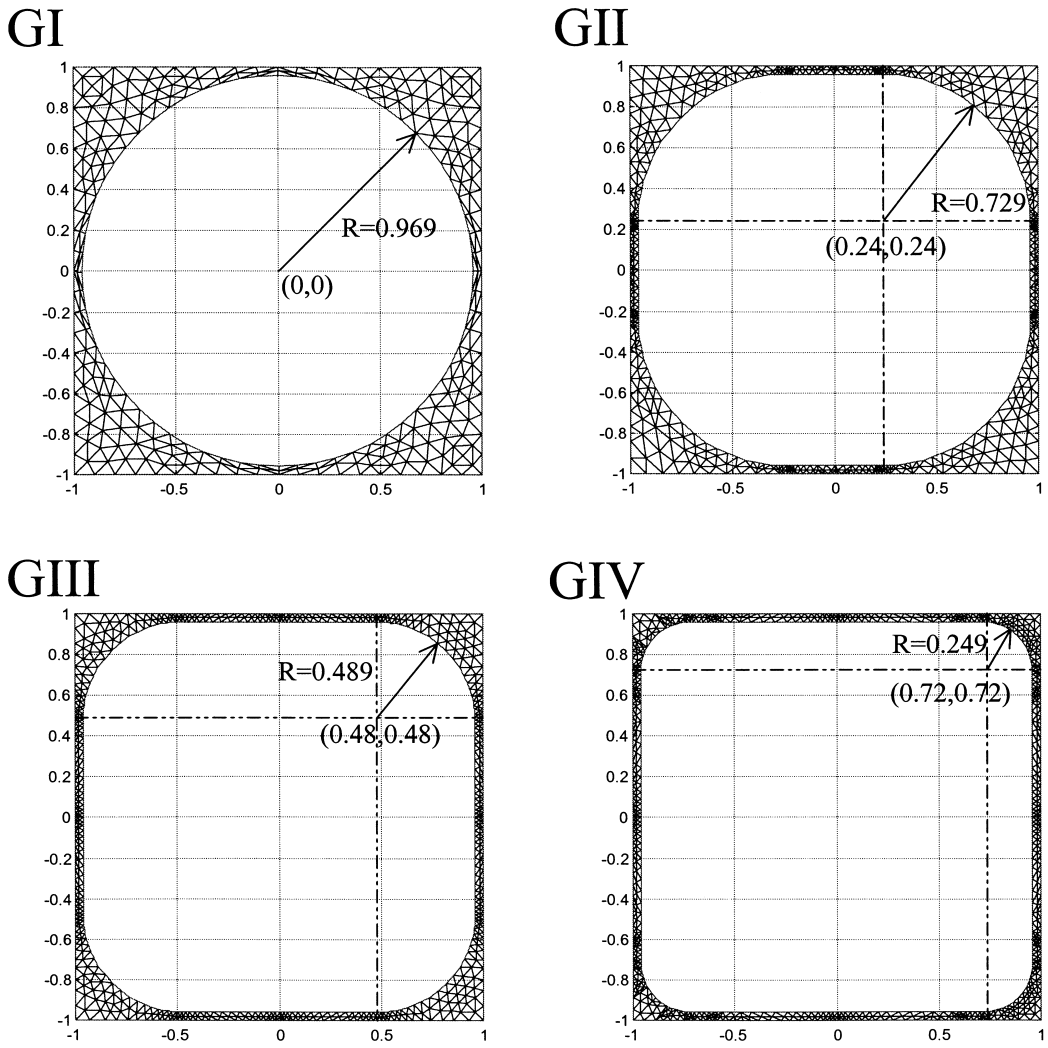

Fig. 1. Dimensionless cross-section and radius of the washcoat geometries. The width of the monolith channel measures 1.25×1.25 mm.

The velocity profiles for the different channel geometries were solved separately from the reduced momentum equations [10]. The correct pressure gradient for a given mean inlet velocity was back iterated using a least-squares procedure. Local Sherwood numbers were calculated from cupmix and peripheral average properties of the channel cross-sections according to the following equation:

$$Sh = \frac{d_h}{(\overline{C}_w - C_b)} \frac{\overline{\partial C}}{\partial n} \quad (4)$$

2.2. Simplified 3D-model based on sectioning the washcoat

Except for the above mentioned conditions for the gas-phase modelling, this particular case reduces the washcoat equations into boundary conditions based on the following assumptions:

- the wall periphery can be divided into small washcoat sections;
- each section can be considered a separate particle as a boundary condition;

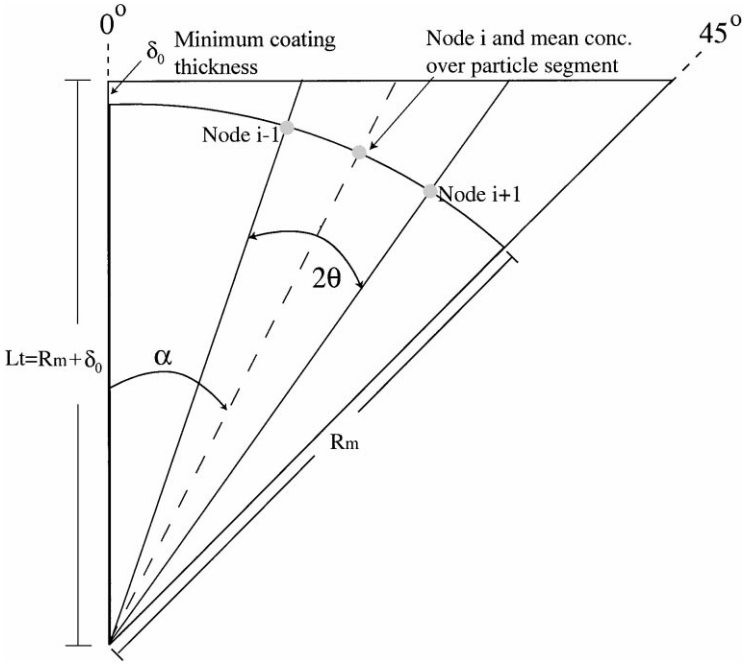

Fig. 2. Discretisation of the washcoat into particles. Figure denotes the simplest geometrical configuration, circle in a square.

- the diffusion of material between particles can be neglected;
- the diffusion and reaction in each particle can be treated as a 1D problem.

The general division of the washcoat characteristic length for the reduced 3D-model can be viewed in the schematic Fig. 2, showing the simplest geometry, GI ("circle in a square"). The characteristic length for a specific node, *i*, is calculated as the volume of the particle divided by the external surface in contact with the channel flow, following the theory of Aris [11]. The segment particle is defined by using the adjacent nodes giving a segment with an angle of 2Θ. The segmentation lines are drawn from the centre of the monolith channel.

The effectiveness factor for such a particle and for the kinetics investigated can be calculated according to the formula for an infinite slab. Here, the thickness of the slab is substituted by the characteristic length of the particles in the generalised Thiele modulus expression [12–15]. Thus, the boundary condition for the reduced 3D-model as a function of the wall periphery becomes

$$\frac{\partial \Psi}{\partial n} = -\frac{\eta(x,y)k_{c0}\delta(x,y)R_m C_{f0}^{n-1}}{D_g}\Psi^n, \quad \eta(x,y) = \frac{\tanh[\Phi(x,y)]}{\Phi(x,y)}, \quad \Phi(x,y) = \delta(x,y)\left(\frac{1}{2}(n+1)\frac{k_{c0}C_{f0}^{n-1}}{D_e}\Psi^{n-1}\right)^{1/2} \tag{5}$$

Depending on the boundary discretisation, the characteristic length for each node, $\delta(x,y)$, will converge towards an asymptotic value if enough boundary nodes are used. For small angles (2Θ) the characteristic length will converge towards an asymptotic value. For instance, if we consider the simplest geometrical configuration a "circle in a square" type of geometry, see Fig. 2, and look for the node particle *i* with an angle of α, the washcoat area to perimeter ratio is

$$\delta(i) = \frac{\frac{1}{2}Lt^2[\tan(\alpha+\Theta) - \tan(\alpha-\Theta)] - R_m^2\Theta}{2R_m\Theta} \tag{6}$$

with symbols as viewed in Fig. 2. When the angle (2θ) is approaching 0, Eq. (6) according to l'Hospital's rule becomes

$$\lim_{\Theta\to 0}\frac{f(\Theta)}{g(\Theta)} = \left[\frac{0}{0}\right] = \lim_{\Theta\to 0}\frac{f'(\Theta)}{g'(\Theta)} = \frac{Lt^2(1+\tan^2(\alpha)) - R_m^2}{2R_m} \quad (7)$$

The above limit function (7) is valid for geometry GI in Fig. 1 and was used as a convergence criterion to investigate how many boundary nodes are needed to obtain a limit of the characteristic length. The characteristic length rapidly converges towards the asymptotic case and with around 50 boundary nodes, the difference is almost negligible in comparison with Eq. (7). This is also the case for all other geometries. Here, the convergence criterion was a large number of boundary discretisations. Note that when the characteristic lengths are approaching their limiting values, the boundary condition (5) approaches towards its limiting value as well, since it is solely depending on $\delta(x,y)$ for convergence.

2.3. Model validation and numerical solution

For the numerical computations of the above DAE-equations, the software Femlab from Comsol AB was used utilising the Galerkin method with linear basefunctions of finite element type. The finite element grid was applied on one octant of the monolith geometry due to symmetry conditions. For all geometric configurations, a uniform mesh of 1800 node points for the gas-phase and 3800 nodes for the solid-phase was enough for convergence. When the temperature was higher with sharp concentration gradients in the solid-phase, a non-uniform mesh with more refinements for the solid, near the exposed washcoat surface, was used (1800 nodes for the gas-phase and 5800 nodes for the solid). It was convenient to integrate the DAE-equations along the axial direction with a backward Euler method of first order accuracy. Hundred uniform axial steps gave almost identical results as when using a higher order method with an adaptive step-control routine (ode15 s in Matlab 5.3).

In order to validate the model equations, the 3D-model was solved for a cylindrical geometry with a flat, uniform, coating along the wall periphery. The results were identical to those of a 2D-model solved with finite differences. Asymptotic Sherwood numbers calculated with the 3D-model for a circular geometry showed less than 0.5% deviation from literature values.

For the reduced 3D-model, the gas-phase equation was dicretised as mentioned above. Enough boundary points assured convergence of the boundary perimeter as discussed in Section 2.2.

3. Results and discussion

3.1. Comparisons between 3D-models

Pre-exponential factors and activation energies for the kinetics investigated are shown in Table 1. For all geometric configurations and kinetic expressions that were used in this study a series of inlet temperature ramps were simulated, covering a temperature interval from 100 to 500°C. This temperature interval covered effectiveness factor values from 1 at low temperatures to about 0.1 at the highest temperature.

In Fig. 3, the outlet conversions as function of temperature are compared for both the rigorous and the simplified 3D approach. The figure shows the results for a 0.7th order reaction rate and for all the geometrical configurations of the monolith matrix. The rigorous 3D-model with equations for both phases is denoted as 3D-(2domain) and the simplified method based on reducing the washcoat into boundary conditions is denoted as 3D-(1domain). The error introduced by the simplified 3D-model is very small when compared with the rigorous model. There is a slight deviation at intermediate temperatures for the geometries with an extreme washcoat thickness at the monolith corner. The approximate method neglects the diffusion of material between the particle segments which in practice occurs to a certain extent.

Table 1
Pre-exponential factors and activation energies

Rate law	Parameter	Value	Exponent
First order	K_1	2.0	10^9
	E_s	7.5	10^4
Power law (0.7th order)	K_1	6.3	10^9
	E_s	8.4	10^4

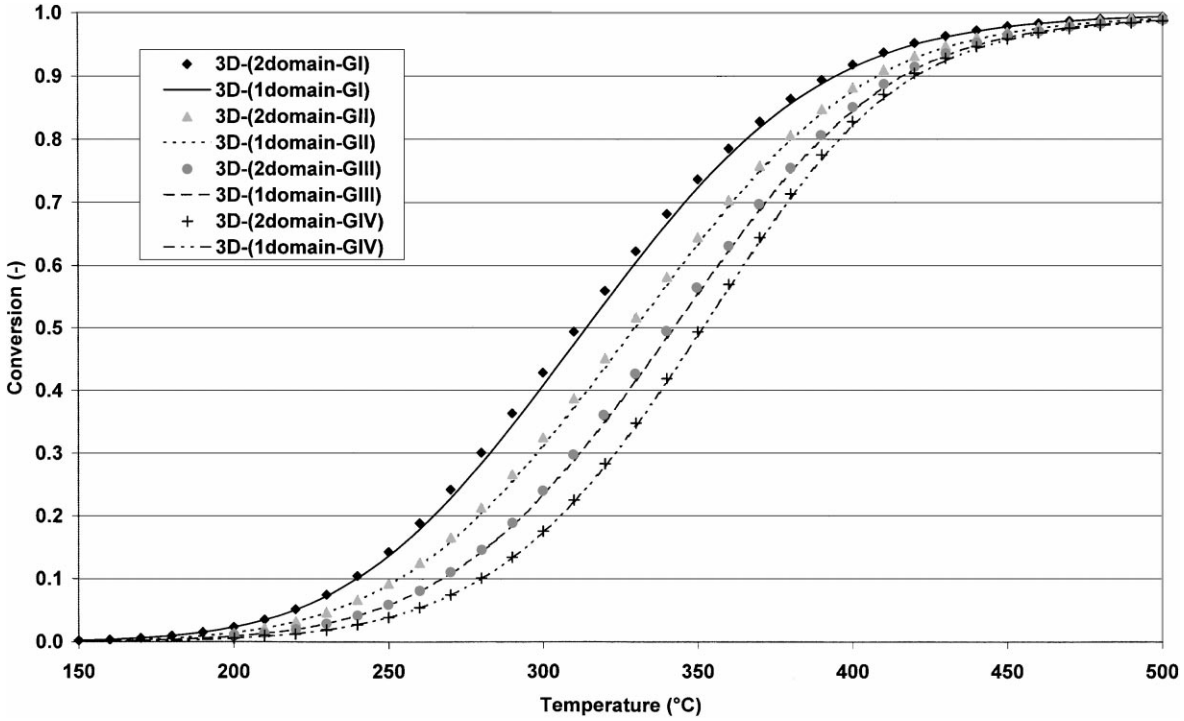

Fig. 3. Conversions calculated by the simplified and the rigorous 3D-models for a 0.7th order reaction and for all geometries. Parameters: L=5 cm, $\bar{U}_0$=2 m s^{-1}, R_m=0.625 mm, P=1 atm, D_{g0}=1 cm^2 s^{-1}, D_e=0.023 cm^2 s^{-1}.

The above results are in line with our previous study for a two-dimensional flow field for the monolithic matrix [9]. The concentration gradient fields have different directions from the divisional lines of the particle segments and deviate more noticeably close to the monolith wall. At intermediate effectiveness factors, the gradient deviation is more pronounced and differs more for the geometries with thicker fillets. However, the division method is successful in the front part of the washcoat surface where a significant reaction occurs. In the part of the washcoat close to the monolith wall, the divisional line and the gradient have different directions but the reaction rate is low and becomes less significant.

Thus, in spite of the concentration differences inside the washcoat, the simplified 3D-model succeeds in reproducing results satisfactorily. For the worst cases with GI and GII as geometrical configurations, the simplified method showed not more than 5% deviation of bulk and wall concentration profiles when compared with the rigorous method. For the rest of the geometries the error was negligible. Similar results were also obtained using a first order reaction rate.

The simplified 3D-model reduced the computer time by a factor of 4–6 in comparison with the rigorous method. However, more significant computer time savings can be obtained whenever cases with multiple reactions have to be investigated.

3.2. Comparison of 3D solutions with 2D and 1D models

To address further computational reductions, both 2D- and 1D-models have been compared with results from the simplified 3D-model. In spite of the non-symmetrical geometries of the monolithic matrices, the 2D-model is used for two reasons: (a) a common practice in literature is that since the washcoat rounds the corners of square monolith, a cylindrical geometry can be assumed using a hydraulic radius, (b) the need for a priori mass transfer correlations does not exist in the two-dimensional case.

For the 2D-model, the gas-phase mass-balance according to Eq. (1) is reduced to cylindrical coordinates. Since we now consider a uniform concentration at the wall periphery, the effectiveness factor can be calculated, as was done in our previous study, with the expression

$$\eta = \sum w_i \eta_i \tag{8}$$

Here, η_i denotes the effectiveness factor of one particle segment of the washcoat and w_i the corresponding segment's mass fraction. The boundary condition is similar to Eq. (5), thus $\eta(x,y)$ may be replaced by Eq. (8) and the characteristic length, $\delta(x,y)$, by the whole volume to surface ratio of the washcoat. This two-dimensional model is defined as (2D-P) in the discussion below.

The one-dimensional model based on average distributions over the cross-section geometry is given by

$$\begin{aligned}
&\text{Gas-phase}: \quad \frac{\overline{U}_0}{L}\frac{\partial \Psi}{\partial z} + \sigma K_\mathrm{f}(\Psi - \Omega) = 0,\\
&K_\mathrm{f} = \frac{Sh(z) D_\mathrm{g}}{d_\mathrm{h}}\\
&\text{Solid-phase}: \quad K_\mathrm{f}(\Psi - \Omega) = \eta k_{\mathrm{c}0} \delta C_{\mathrm{f}0}^{n-1} \Omega^n,\\
&K_\mathrm{f} = \frac{Sh(z) D_\mathrm{g}}{d_\mathrm{h}}
\end{aligned} \tag{9}$$

where the effectiveness factor is calculated according to Eq. (8). The validity of the one-dimensional model depends on good correlations for the mass-transfer coefficient, K_f. The choice of proper correlations for the interphase transfer coefficients in monolithic channels has been discussed in a number of works in literature [16–18]. Here, we use local Sherwood numbers for a complete diffusional regime (analogy to the Graetz–Nusselt problem with constant wall temperature, Nu_T) in order to evaluate the mass transfer coefficient. Such an approach was used by Tronconi and Forzatti [18] to model SCR monolith reactors in absence of pore effects. A very good agreement was found by the authors between the 1D model and the equivalent multidimensional ones.

Asymptotic values of Sherwood numbers are shown in Table 2 for the geometrical configurations in this study. The values are calculated for two limiting cases: (a) according to the analogy of the Graetz–Nusselt problem with constant wall temperature, $Sh_\infty(Nu_T)$, and (b) according to the same thermal analogy but for constant axial wall heat flux with uniform peripheral wall heat flux, $Sh_\infty(Nu_{\mathrm{H}2})$ [19]. The latter case is valid for a wholly kinetically limited regime.

Table 2
Asymptotic Sherwood numbers for the geometries investigated

Geometry	Sherwood numbers in this work		Literature values [19]	
	$Sh_\infty(Nu_{\mathrm{H}2})$	$Sh_\infty(Nu_T)$	$Sh_\infty(Nu_{\mathrm{H}2})$	$Sh_\infty(Nu_T)$
GI (cylindrical)	4.369	3.670	4.364	3.657
GII	4.281	3.623	–	–
GIII	4.040	3.506	–	–
GIV	3.659	3.304	–	–
Square	3.093	2.977	3.091	2.976

Fig. 4(a) and (b) shows the outlet conversion for the highest inlet temperatures for the different models and for 0.7th order reaction. The conversions at low temperatures, not shown here, are almost identical for all models since kinetics rather than mass-transfer effects controls the overall process. At higher temperatures, when mass-transfer resistances are more elevated, a difference between the models can be observed. In Fig. 4(a), showing results for the GII-geometry, the conversion for the 2D-P model is in agreement with the simplified 3D-model, while the one-dimensional model slightly underestimates the results. The GII-geometry with thick washcoat fillets show an asymptotic Sherwood number close to the value for the cylindrical case, see Table 2. The two-dimensional model therefore imposes correctly the flux-boundary condition for this geometry. As the fillet radius of the washcoat is decreased in the other geometries, the asymptotic Sherwood numbers also decrease and progress towards the limiting value for a square channel. For the GIV-geometry, the 2D-P model now overpredicts the conversion compared to the simplified 3D-model, as expected, see Fig. 4(b). The variance in the results is reflected by the difference in the Sherwood numbers between the two-dimensional model and the real value for this geometry.

The slight underestimation of the conversion obtained with the 1D-model is due to the reaction not being totally limited by kinetics which is implied by the local Sherwood number we use. However, the difference is small and differs only in a region when both kinetics and interphase mass transfer resistances are

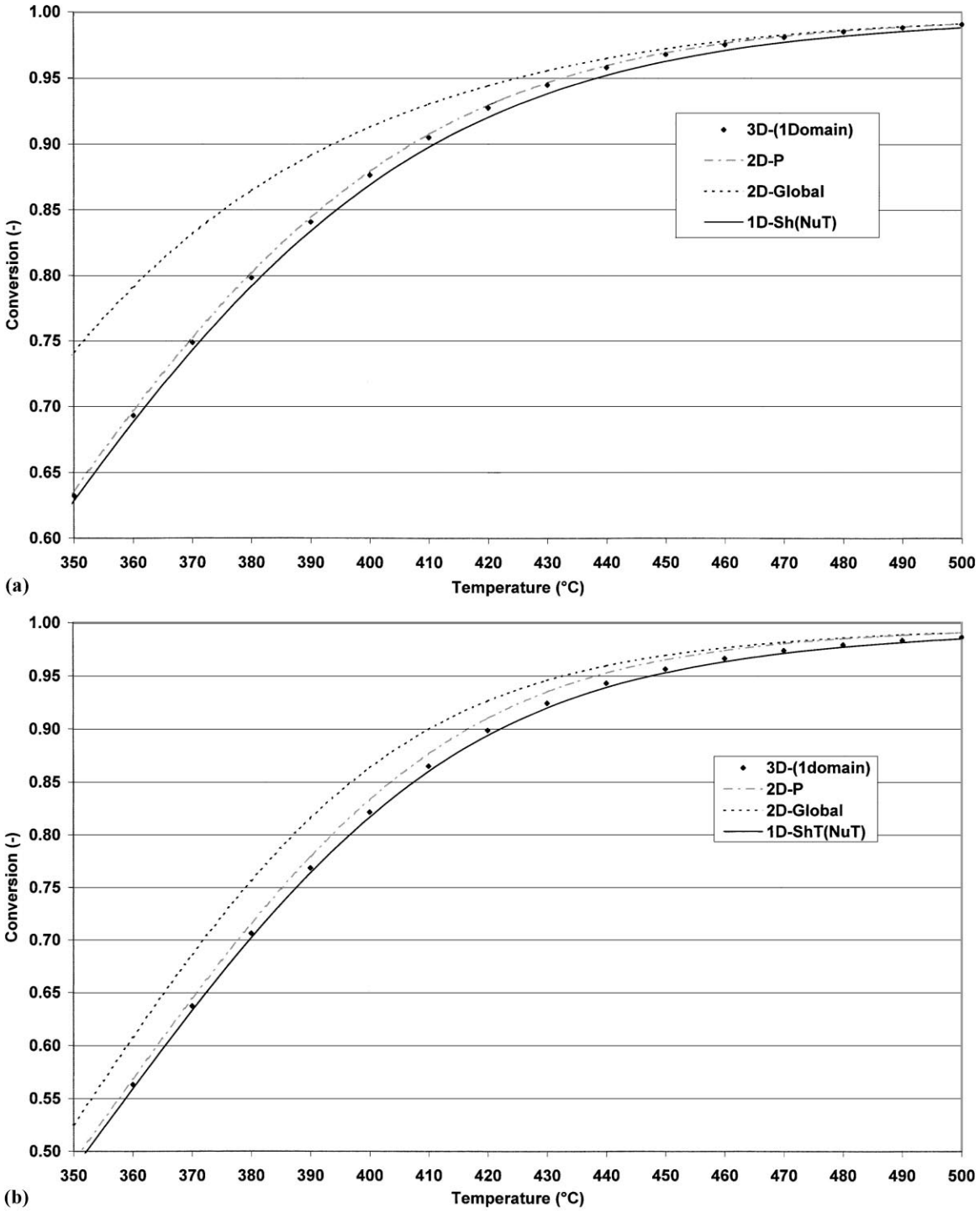

Fig. 4. (a)–(b) Conversions for the highest temperatures and for 0.7th order reaction. Calculated conversions are compared using different kinds of models. Parameters: L=5 cm, $\bar{U}_0$=2 m s^{-1}, R_m=0.625 mm, P=1 atm, D_{g0}=1 cm^2 s^{-1}, D_e=0.023 cm^2 s^{-1}. (a) GII-geometry, (b) GIV-geometry.

of the same magnitude. Note that an even better agreement can be obtained for the mass-transfer coefficient if a formula interpolating between Nu_{H2} and Nu_T is used in Ref. [16].

We also want to point out the danger of using an effectiveness factor based on the whole washcoat as one particle. This extreme case of treating the effectiveness factor using a global characteristic length is investigated using a 2D-model denoted as (2D-G).

As seen in Fig. 4, this approach gives marked differences in the conversions from the other models. The difference is more pronounced for the GII-geometry with thick coating and for intermediate temperatures. However, at the highest temperatures, where most of the reaction takes place near the exposed surface of the washcoat, the effectiveness factors converge to the exact asymptotic expression ($\eta=1/\Phi$) and there is therefore no difference between the two bidimensional models [15].

As a final remark, it should be stressed that the simpler dimensional models, especially the 1D-model, may not be accurate in cases when LHHW-kinetics with strong inhibiting effects or adiabatic conditions are investigated. Such cases show marked changes in Sherwood and Nusselt numbers in the vicinity of the light-off position and depend much on the geometrical configuration [16]. Here, the reduced 3D-model is general for such cases and can still give significant computational reductions. This case is however beyond the scope of the present study and will not be treated further in this paper.

4. Nomenclature

C_b average cupmix concentration (mol m^{-3})
$\bar{C}_w$ average peripheral wall concentration (mol m^{-3})
C_{f0} inlet concentration (mol m^{-3})
D_e effective diffusivity (m^2 s^{-1})
D_g molecular diffusion coefficient $D_{g0}(T/723)^{1.75}$ (m^2 s^{-1})
d_h hydraulic diameter of monolith channel (m)
E_s activation energy (J mol^{-1})
k_{c0} intrinsic rate constant (various units)
K_1 pre-exponential factor for first order reaction (s^{-1})
K_2 pre-exponential factor for 0.7th order reaction (mol$^{0.3}$ m$^{-0.9}$ s^{-1})
K_f mass-transfer coefficient (m s^{-1})
L channel length (m)
L_c characteristic length, ratio of catalyst volume to surface area (m)
n reaction rate order in power law kinetics
P pressure (atm)
R dimensionless radius for washcoat geometry
R_m maximum length in the monolithic channel (m)
$Sh(z)$ local Sherwood number
T temperature (K)
U axial velocity (m s^{-1})
$\bar{U}_0$ average cupmix velocity at STP (m s^{-1})
w_i mass fraction of particles of size i
x dimensionless x-coordinate
y dimensionless y-coordinate
z dimensionless axial-coordinate

Greek letters
δ thickness of active catalyst layer, volume to surface ratio (m)
η_i effectiveness factor for particles of size i
η effectiveness factor, average effectiveness factor
σ ratio of wetted perimeter to cross-sectional area (m^{-1})
Φ Thiele modulus
Ψ dimensionless concentration (gas-phase concentration for 1D-model)
Ω dimensionless wall concentration for 1D-model

5. Conclusions

1. A general and less numerically expensive 3D-model based on segmenting the washcoat into particles showed good agreement with a more rigorous model for first order and power-law kinetics.
2. Accurate results for the kinetics studied and for isothermal conditions could also be obtained with simpler models based on proper approximations for the effectiveness factor. A 1D-model based on properly evaluated mass-transfer coefficients could be used to model all the geometrical configurations. However, a 2D-model may give

overoptimistic results especially in cases with a less rounded washcoat thickness.

Acknowledgements

Funding from the Swedish National Energy Administration (formerly NUTEK — the Swedish National Board for Industrial and Technical Development) is gratefully acknowledged. We wish to thank our colleague Christina Hörnell for her suggestions and helpful discussions.

References

[1] H. Bosch, F.J. Janssen, Catal. Today 2 (1988) 369.
[2] A. Cyboulski, J.A. Moulijn, Catal. Rev. Sci. Eng. 36 (1994) 179.
[3] E.M. Johansson, D. Papadias, P.O. Thevenin, A.G. Ersson, R. Gabrielsson, P.G. Menon, P.H. Björnbom, S.G. Järås, Catalysis-Specialist Periodical Reports, Vol. 14, Royal Society of Chemistry, Cambridge, 1999, p. 183 (Chapter 6).
[4] A. Nakjhavan, P. Björnbom, M.F.M. Zwinkels, S.G. Järås, Chem. Eng. Sci. 50 (1995) 2255.
[5] L.C. Young, B.A. Finlayson, AIChE J. 22 (1976) 331.
[6] G. Groppi, A. Belloli, E. Tronconi, P. Forzatti, AIChE J. 41 (1995) 2250.
[7] C. Chou, W.E. Stewart, Chem. Eng. Sci. 41 (1986) 202.
[8] D. Leung, R.E. Hayes, S.T. Kolaczkowski, Can. J. Chem. Eng. 74 (1996) 94.
[9] D. Papadias, L. Edsberg, P. Björnbom, Chem. Eng. Sci. 55 (2000) 1447.
[10] R.B. Bird, W.E. Stewart, E.N. Lightfoot, Transport Phenomena, Wiley, New York, 1960, p. 84 (Chapter 3).
[11] R. Aris, Chem. Eng. Sci. 6 (1957) 262.
[12] R. Aris, Ind. Eng. Chem. Fund. 4 (1965) 227.
[13] K.B. Bischoff, AIChE J. 11 (1965) 351.
[14] E.E. Petersen, Chem. Eng. Sci. 20 (1965) 587.
[15] O. Levenspiel, Chemical Reaction Engineering, 2nd Edition, Wiley, New York, 1972, p. 478 (Chapter 14).
[16] G. Groppi, E. Tronconi, P. Forzatti, Catal. Rev. Sci. Eng. 41 (1999) 227.
[17] R.E. Hayes, S.T. Kolaczkowski, Introduction to Catalytic Combustion, Gordon and Breach, Amsterdam, 1997, p. 313 (Chapter 3).
[18] E. Tronconi, P. Forzatti, AIChE J. 38 (1992) 201.
[19] R.K. Shah, A.L. London, Laminar Flow Forced Convection in Ducts, Academic Press, New York, 1978, p. 394 (Chapter 17).